DEVELOPMENTAL DYNAMICS 236:802–809, 2007

TECHNIQUES

Quantitative Volumetric Analysis of Cardiac Morphogenesis Assessed Through Micro-Computed Tomography

Jonathan T. Butcher,[1]* David Sedmera,[1] Robert E. Guldberg,[2] and Roger R. Markwald[1]

We present a method to generate quantitative embryonic cardiovascular volumes at extremely high resolution without tissue shrinkage using micro-computed tomography (Micro-CT). A CT dense polymer (Microfil, Flow Tech, Inc.) was used to perfuse avian embryonic hearts from Hamburger and Hamilton stage (HH) 15 through HH36, which solidified to create a cast within the luminal space. Hearts were then scanned at 10.5 μm^3 voxel resolution using a VivaCT scanner, digital slices were contoured for regions of interest, and computational analysis was conducted to quantify morphogenetic parameters. The three-dimensional morphology was compared with that of scanning electron microscopy (SEM) images and serial section reconstruction of similarly staged hearts. We report that Microfil-perfused hearts swelled to maximum end-diastolic volume with negligible shrinking after polymerization. Comparison to SEM revealed good agreement of cardiac chamber proportions and intracardiac tissue structures (i.e., valves and septa) at the stages of development assessed. Quantification of changes in chamber volume over development revealed several notable results that confirm earlier hypotheses. Heart chamber volumes grow over two orders of magnitude during the 1-week developmental period analyzed. The atrioventricular canal comprised a significant proportion of the early heart volume. While left atrium/left ventricular volume ratios approached 1 in later development, right atrium/right ventricle ratios increase to over 2.5. Quantification of trabeculation patterns confirmed that the right and left ventricles are similarly trabeculated before HH27, after which the right ventricle became quantitatively coarser than that of the left ventricle. These results demonstrate that Micro-CT can be used to image and quantify cardiovascular structures during development. *Developmental Dynamics 236:802–809, 2007.* © 2006 Wiley-Liss, Inc.

Key words: development; heart; chamber; Micro-CT; volume; embryo

Accepted 16 August 2006

INTRODUCTION

Embryonic heart morphogenesis is a complex and dynamic process that is incompletely understood, but critically important for long-term survival. The heart begins as a linear tube of myocardium lined with endocardial cells that functions like a suction pump (Forouhar et al., 2006), but quickly loops and grows into a four-chambered heart complete with valves and septa that pumps in a piston manner. This process involves several key events that happen in three dimensions, including linear heart tube looping, septation of the ventricles, and development of the atrioventricular (AV) valve apparatus, defects in which result in a myriad of clinically relevant congenital heart defects (Collins-Nakai and McLaughlin, 2002; Gittenberger-de Groot et al., 2005). Although the initial heart tube only contains portions of the primitive right ventricle (de la Cruz et al., 2001), eventually all of the chambers are derived from the growing linear

[1]Cardiovascular Developmental Biology Center, Department of Cell Biology and Anatomy, Medical University of South Carolina, Charleston, South Carolina
[2]Petit Institute for Bioengineering and Bioscience, Georgia Institute of Technology, Atlanta, Georgia
Grant sponsor: NIH; Grant number: T32 H2007710; Grant number: HL52813; Grant number: HL33756.
***Correspondence to: Jonathan T. Butcher, Department of Cell Biology and Anatomy, Medical University of South Carolina, Basic Science Building Room 601, 173 Ashley Avenue, Charleston, SC 29425. E-mail: butchej@musc.edu**

DOI 10.1002/dvdy.20962
Published online 29 September 2006 in Wiley InterScience (www.interscience.wiley.com).

© 2006 Wiley-Liss, Inc.

heart tube, with smaller contributions from sources such as the anterior heart field and proepicardium. During cardiogenesis, the sizes of these chambers change significantly, but few studies have attempted to quantify them. Two studies by Wenink's group in the 1990s quantified chamber-specific myocardial tissue volume changes over development using a point counting method and found that over two orders of magnitude of heart growth occurs in the embryonic rat and human (Wenink, 1992; Knaapen et al., 1995). It is unclear, however, how the lumen volumes of the different segment/chambers change during development. Studies by Keller et al. have attempted to quantify ventricular volumes at different stages of development and showed that these increase in size as the embryo grows, but how these volumes relate to those of the atria and outflow tract were not assessed (Keller et al., 1996).

Many details of cardiac morphogenesis are only now being uncovered in part because of the complexities of the developing geometries. The human heart becomes four chambered by week 8, which is approximately the same time that the embryo can be visualized through ultrasound and, therefore, too late for detailed morphogenic study (Zimmer et al., 1994; Fong et al., 2004). Therefore, embryonic animal models, particularly chick and mouse, have been essential for these investigations. One particular challenge, however, is the extremely small size of these hearts and the rapidity in which they develop. The pumping linear heart tube appears at Hamburger and Hamilton stage (HH) 12 in the chick (approximately 48 hr of incubation) and generally resembles its mature configuration by HH36 (day 10), or E8.5 to E16.5 in the mouse. Additionally, these hearts are microscopic throughout the developmental window, forcing researchers to use alternate means to visualize these events. Typically, en face microscopic images, scanning electron microscopy (SEM), optical scans, and histological sectioning have been used to describe aspects of morphogenesis, but each has its drawbacks. Photographic images, even with scales, do not have the capacity to measure depth, limiting their utility for three-dimensional (3D) quantification. The 3D serial reconstruction using histological sections has dramatically improved understanding of heart development with the ability to combine geometry and the expressions of cell and/or matrix proteins (Moorman et al., 2000; Groenendijk et al., 2005). However, accuracy of this process is extremely sensitive to the number of sections processed, limiting its use to research labs with specifically dedicated technicians and equipment. Even so, the ability to render complex, high-curvature 3D structures such as developing valves is limited with this technique because of the single sectioning plane used and the amount of subjectivity required to manually align sections. Optical scanning techniques have also been used to render 3D and 4D volumes of early heart geometries (Liebling et al., 2005; Jenkins et al., 2006), but penetration depth limitations with this technique require imaging early stages and/or using optically clear specimens or preparations.

While the exterior walls of the heart are generally smooth with large radii of curvature, the interior "lumens" of the heart, with varying trabecular, septal, and valvular geometries, are far more complex. It is through this lumen that hemodynamic forces (wall shear stress, blood pressure) interact with developing tissue surfaces. Few studies to date have attempted to profile the changing geometry of the interior of the heart. Several studies have used different imaging modalities to explore developing hearts in 3D to identify morphogenic defects (Smith, 2001; Weninger and Mohun, 2002; Schneider et al., 2003; Soufan et al., 2004), but none of these studies focused on quantifying the 3D geometry of the different segments and chambers.

Quantification of changing heart chamber volumes would provide insight into the changing function of the early heart, but different imaging technologies may be required to accomplish this in these microscopic tissues. One technique that has been used over the past 15 years to quantify complex geometries at small resolutions is micro-computed tomography (Micro-CT). Micro-CT works by scanning a subject with high-powered X-rays and rendering the dense regions in a volume. The scan head is rotated 360 degrees around the subject, developing a near continuous series of planar slices with no registration defects. Voxel sizes less than 10 μm are readily achievable with Micro-CT (Guldberg et al., 2003), which is superior to those currently achievable with ultrasound (30 μm) and magnetic resonance imaging (100 μm). Micro-CT has mainly been used for visualizing and quantifying bone architecture and development (Guldberg et al., 2004), and several studies have been conducted using this technique to quantify trabecular structures (Chappard et al., 2006). More recent studies using radio-opaque contrast agents have enabled the visualization of microvascular structures, such as those associated with bone fracture healing (Duvall et al., 2004) and coronary artery vasa vasorum (Gossl et al., 2004).

We, therefore, hypothesized that Micro-CT could be used to visualize and quantify the changing cardiac lumen during embryonic development. Our objectives, therefore, were to compare the visualization of the heart lumen using Micro-CT with serial section reconstruction and scanning electron microscopy, measure the volume of each developing segment/chamber from HH15 through HH36, and determine the 3D structure of the developing atrioventricular valves.

RESULTS

Perfusion and Polymerization

Perfusion of embryonic chick hearts was accomplished through a combination of vitelline and ventricular microneedle injections (Fig. 1), which resulted in polymerized CT dense gels forming in the luminal space of cardiovascular structures. The Microfil polymer was nonmixing and, therefore, excluded blood wherever it went without being diluted. It was critical to culture the embryos ex ovo in the weigh boat humidified chambers to maintain normal development while preserving vitelline vein integrity for perfusion. Perfusion of beating hearts was monitored and flow-rate adjusted by changing the height of the syringe and the diameter of the microneedle to ensure no overfilling of the chambers or premature polymerization. Polymer-

ization of the agent did not result in any additional contraction or expansion, preserving consistently dilated hearts as determined by the perfusion conditions and embryonic stage. Micro-CT scanning of the complete embryos shows that the internal structures of veins and vessels connected to the heart were also preserved using these techniques. Embryos as early as HH15 and as late as HH37 could be perfused in a well-controlled manner using these techniques. Maintaining the integrity of as much of the extraembryonic vasculature as possible was critical to the success of the perfusion, because the hydraulic resistance of these vessels limited the amount of shunting that could cause incomplete perfusion. The polymer: catalyst:diluent concentrations could be modified to delay or speed up the polymerization reaction. We found that combinations involving more than 25% polymer or 10% catalyst resulted in rapid polymerization within the microneedle, whereas polymer percentages under 5% resulted in no cast formation. Thus, the ratios developed in this study can be used to effectively perfuse embryonic heart structures, but additional modifications are possible for the investigation of other cardiovascular structures.

Comparisons Between Techniques

The Micro-CT–generated lumen volumes of staged chick hearts were then compared with 3D serial reconstructions and frontal SEM images (Fig. 2). SEM images show the looped heart at HH16, development of trabeculation and atrioventricular cushion outgrowth at HH23, and almost completely septated atria and ventricles by HH30. Although each image provides true in situ lumen and wall structural organization at submicrometer resolution, these hearts also have collapsed atrial folds, do not permit visualization without tissue destruction, and experience approximately 20% volumetric shrinkage as a result of the processing techniques required. The 3D reconstruction of 2D serial histological sections also creates heart volumes that reflect the inconsistent geometry that results from fixation, embedding, and sectioning procedures. The atria and ventricles of any stage analyzed were regularly in an undefined state of contraction, creating variability in lumen geometry that may not be recognized by analyzing the exterior of the heart. The accuracy of 3D reconstruction was also highly dependent on the plane of sectioning. Frontal sections were best for determining atrial and ventricular lumens as well as atrioventricular valve shape, whereas sagittal sections were better for outflow tract geometries. It is important to note that greater numbers of sections can be used to reconstruct hearts to achieve higher resolution, but the same processing artifacts will persist and the time and expense increase linearly. The 50-μm section spacing we used resulted in similar processing times in comparison to the complete Micro-CT scanning.

Micro-CT generated lumen volumes were derived from perfused hearts that were maintained in their maximally dilated configuration by the polymer cast, thus preserving accurate anatomical structures (Fig. 2). Micro-CT of HH16 hearts show the single atrial chamber, atrioventricular canal, single ventricle, and outflow tract with more physiologically inflated volumes than with serial reconstruction. A virtual frontal plane section shows lumen structure and course comparable to SEM. HH23 hearts accurately show the 3D atrioventricular cushion structure, surface trabeculation, and the growth of the interventricular septum similar to what is observed by SEM, and more accurately than the serial reconstruction. Comparing HH30 Micro-CT hearts with serial section reconstruction hearts shows that Micro-CT more accurately depicts complex 3D shapes such as septa and valves, with structure similar to what is observable in SEM images. Taken together, these results demonstrate the efficacy of Micro-CT in generating embryonic cardiac volumes.

Quantification of Chamber Volumes

Micro-CT was also used to quantify the lumen volume of cardiac structures (Fig. 3). We measured the volume of cardiac segments and chambers from HH15 through HH36 using well-established morphological markers of segment/chamber boundaries (i.e., indentations, septa, valves, etc.). At HH15, the average volume of the atrium, AV canal, and ventricle are almost identical at 0.06–0.066 mm,^{3} with the average outflow tract lumen volume much smaller at 0.014 mm^3. The size of the heart lumen nearly triples by HH17, and the AV canal volume reduces to approximately half of the atrium or ventricle, which are almost identical at approximately 0.03 mm^3. Between HH15 and HH36, an incubation period of approximately 1 week, the total volume of the heart increases over two orders of magnitude, from 0.021 mm^3 to over 32 mm^3. Initially (HH23, the first stage analyzed with definitive left and right chambers), the left atrium is over three times larger than the left ventricle (3.71 mm^3 vs. 0.92 mm^3, $P < 0.05$), but by HH36, this ratio approaches 1.0 and these volumes are not significantly different (V ~7.3 mm^3, $P = 0.64$). The right atrium–right ventricular (RA–RV) volume ratio, however, evolves distinctly differently. At HH23, the RA is approximately twice the size of the RV (1.44 vs. 0.63 mm^3, $P < 0.05$) but both chambers are roughly half the volume of their left-sided counterparts ($P < 0.05$). Instead of converging, the RA–RV ratio is maintained in three of the four stages of development analyzed (at HH30, RA/RV is 1.25) and becomes 2.5 by HH36. The LA begins approximately 2.3 times larger than the RA, but by HH36, is only 65% the size of the RA. The LV on the other hand maintains a 50% size advantage over the RV throughout the stages analyzed. The AV canal volume disappears by HH27 as the AV valves develop, separating the atria and ventricles. The outflow tract volume was defined as the lumen space extending from the end of the ventricles to the aorticopulmonary septum, and by HH30, this volume is reduced to zero coinciding with the development of the separate aortic and pulmonary outlets.

Development of the Atrioventricular Valves and Septa

As shown in Figure 4, chick atrioventricular valve development was visualized three-dimensionally using Mi-

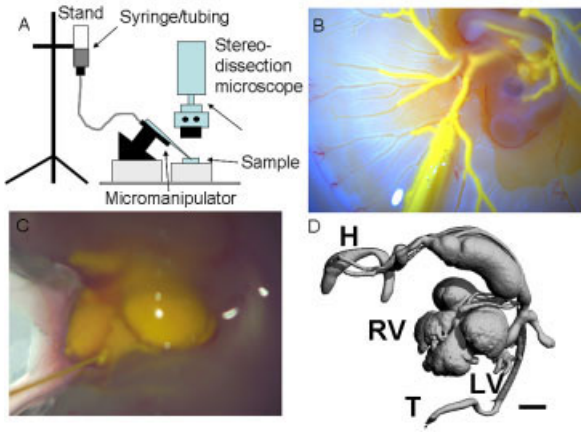

Fig. 1.

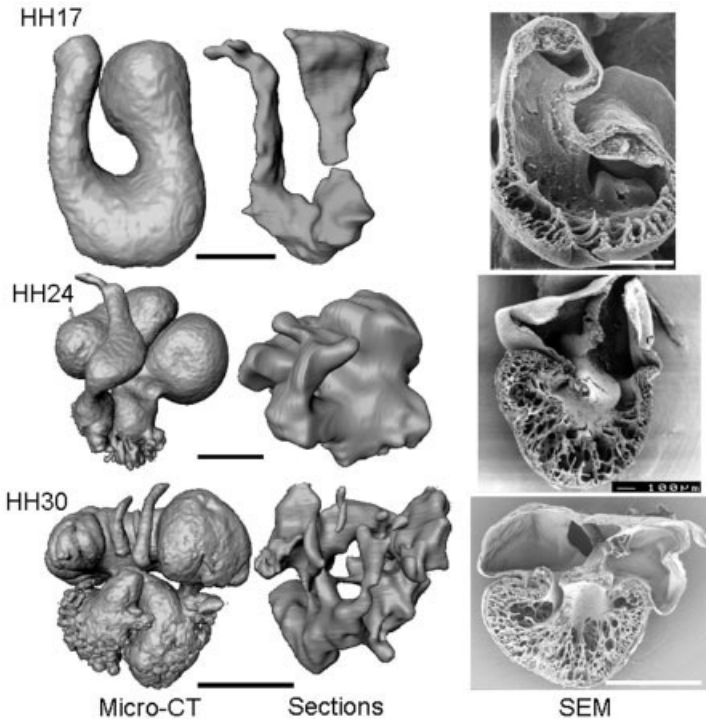

Fig. 2.

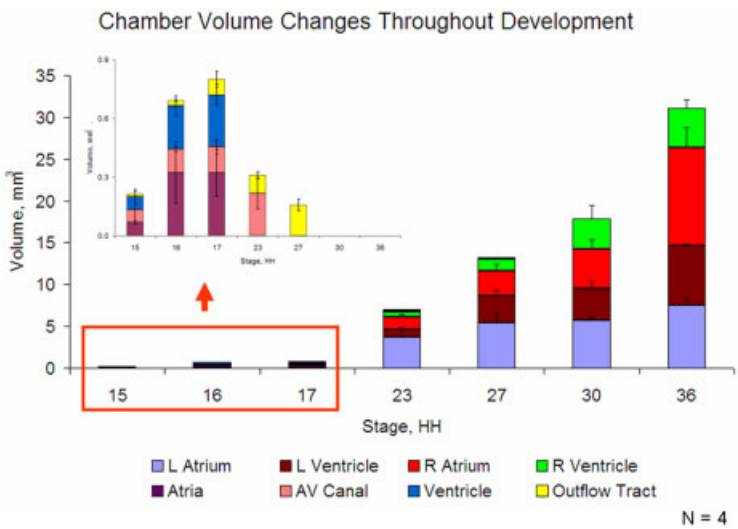

Fig. 3.

cro-CT. At HH16, the AV cushions were only seen as a concave narrowing of the AV canal. Cushion formation was clearly visible by HH23, by which time each atrium had its own connection to the septating ventricle. By HH27, the AV cushions were completely fused, forming a central cushion mass that was very similar in shape to SEM images. The interventricular septum was complete except for the residual interventricular foramen to accommodate blood flow out of the left ventricle, which was shown by Micro-CT virtual section and confirmed by SEM. The septal leaflet of the left AV valve has just begun the process of condensation and elongation, while the mural leaflet has dramatically increased in size over that of HH23. Small fenestrations also appear between the mural cushion and the myocardial wall, which were shown by Micro-CT and confirmed by SEM. Chick hearts were definitively four chambered at HH30, with a completed interventricular septum and separate outflow tracts. Both leaflets of the left AV valve have condensed and elongated further, while the septal leaflet of the right AV valve appears to be absorbed into the septum. The development of the avian right AV muscular flap valve is also clearly visible through virtual sectioning of the Micro-CT volumes. By HH36, the development of the atrioventricular valves is largely complete. The tendinous chord connections between the

Fig. 1. Microfil perfusion system and micro-computed tomography (Micro-CT) rendering of embryonic tissues. **A:** Schematic of the perfusion system. **B:** Microfil perfusion of a Hamburger and Hamilton stage (HH) 25 embryo through a vitelline vein. **C:** Perfusion directly through the ventricle of an HH30 embryo. **D:** Micro-CT rendering of an HH36 embryo, showing the extracardiac vessels that are also perfused. H, head; T, tail; RV, right ventricle; LV, left ventricle. Scale bar = 1 mm.

Fig. 2. Comparison of micro-computed tomography (Micro-CT) scanned hearts (left) with serial section reconstruction (center) and scanning electron microscopy (right). Top = Hamburger and Hamilton stage (HH) 17; Middle = HH23; Bottom = HH30. HH17 and HH23 scale bar = 250 μm. HH30 scale bar = 1 mm.

Fig. 3. Quantification of segment/chamber lumen volumes over development. Insert shows early segment volumes in a relevant scale. Each chamber/segment is represented by its own color. N ≥ 3 samples per stage were analyzed; bars denote standard deviations.

now thin fibrous left AV leaflets and ventricular myocardium can be clearly seen in 3D by means of Micro-CT, as well as the complexities of the leaflet shapes. The interventricular septum has increased in thickness, and the right septal cushion has almost completely disappeared. The pectinate muscles have developed in both the left and right atria, and the right AV flap valve is fully formed. These shapes correspond well to the frontally bisected hearts imaged by SEM.

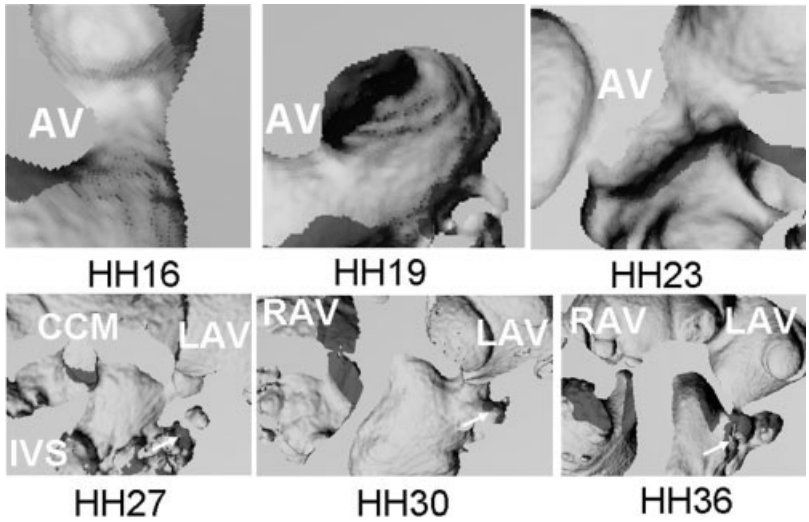

Fig. 4. Virtual frontal plane sections showing the morphological development of the left atrioventricular (AV) valve in three dimensions. Arrows denote the initiation of AV myocardial fenestrations (Hamburger and Hamilton stage [HH] 27) and eventual formation of the chordal supporting apparatus (HH36). Scale bar lengths as indicated.

Formation and Quantification of Ventricular Trabeculation

As seen by Micro-CT, the ventricle wall is largely smooth at HH16. As secondary myocardium is added to these growing pumping chambers, trabeculations appear in the ventricular walls to assist nutrient convection. Initially similar in morphology between the two chambers (see HH23 and HH27), the structure diverges at HH30 and more significantly by HH36. The right ventricle acquires a "coarse" trabeculation pattern, with deep pitting of the ventricular wall, while left ventricular trabeculation becomes more fine. These walls become relatively smooth in comparison, although closer inspection reveals many, more shallow pits in the ventricular wall. These 3D trabeculation patterns were quantified using the computational algorithms developed previously for bone trabeculation (Fig. 5). Initially, the trabecular number, thickness, and spacing, were all similar between ventricles ($P > 0.05$). LV trabecular number decreased over developmental stage concomitant with an increase in trabecular thickness, while spacing remained unchanged. RV trabecular number was maintained between HH23 and HH30, but decreased by HH36, but in this case trabecular spacing increased. It is important to note that, because the CT dense region is the ventricular lumen, therefore, the conceptualization of tissue "thickness" and "spacing" are reversed (i.e., the "tissue" is actually space and vice versa). Therefore, the decrease in trabecular number of the LV chamber volume compared with the RV (1.34 vs. 1.77, $P < 0.05$) suggests more trabeculae are identifiable on the LV wall. The greater LV trabecular thickness compared with the RV suggests that the LV trabeculae are thinner or more fine. The larger RV trabecular spacing number compared with LV suggests that the RV trabeculae are spaced further apart than those of the LV, suggesting that the space between them is more easily identified. Taken together, the changes in these parameters correspond well to the "fine" and "coarse" trabeculation pattern development of the left and right ventricle as reported earlier (Wenink, 1992). The large ventricular cavity corresponds to a solid volume when reconstructed, and current limitations in the software required that this volume be included for trabecular analysis. Quantification without these bolus volumes would, therefore, result in enhanced differences in the measured parameters between the two ventricles.

DISCUSSION

Embryonic cardiac morphogenesis is a complex 3D process that occurs rapidly. Understanding this process necessitates the ability to image these small structures with high resolution with the capacity for morphological quantification. Several techniques have been and are routinely used to observe this developmental process, each with their own advantages and limitations. The results of this study show that Micro-CT can visualize embryonic hearts during a wide range of development at resolutions on the order of 10 μm. The entire scanning process takes approximately 20 min, and the resulting volumes are in complete registration. This finding is an advantage over serial section reconstruction, which often takes weeks to assemble sections of the heart and involves subjectivity in aligning them. In addition, the anisotropy in resolution (planar vs. nonplanar) results in variability between renderings based on in what plane the tissue is sectioned. However, serial section reconstruction can be used in conjunction with immunohistochemistry and/or in situ hybridization to combine morphological information with gene and protein expression, which is not currently possible with Micro-CT. Clinical imaging techniques such as high-frequency ultrasound and magnetic resonance imaging have the capacity to render 3D morphologies in real time, albeit at a much lower resolution (~100 μm or more). CT scanning has been used with gating and contrast agents to monitor changing shapes in vivo, and smaller bubble contrast agents are being developed to permit embryonic research using Micro-CT. These same techniques can be readily applied to

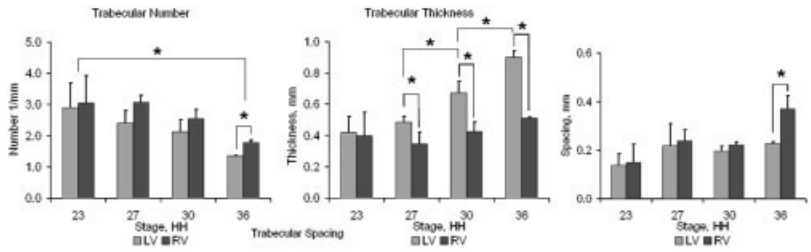

Fig. 5. Quantification and comparison of ventricular trabeculation patterns. Bars denote standard deviations. The asterisk denotes significance at $P < 0.05$.

other injectable embryonic systems, including mouse, frog, and zebrafish.

We used Micro-CT to visualize avian embryonic heart lumens and to quantify the volumes of the heart segments and chambers through the majority of the cardiac developmental window. We found that the heart increases two orders of magnitude in size from HH15 through HH36 over a period of approximately 1 week. Other researchers have shown smaller increases in volume using different techniques. Keller et al. measured ventricular volumes of embryonic mouse hearts from E10.5 to E14.5 using ellipsoid approximations based on 2D area tracings on the outside, and they found that they only double in size over this time (Keller et al., 1996). This finding may reflect differences between mouse and chick, but it is likely that the 2D approximations underestimated actual volumes. Keller et al. found that right ventricular volume was larger than that of the left ventricle over each stage developed, which is in contrast to our study but likely reflects the right ventricular anatomical differences between mouse and chick. Hu and Clark measured atrioventricular filling from HH16 through HH27 and found that this volume increased from approximately 0.06 mm^3 to 0.8 mm^3 (Hu et al., 1991). Combining the volume of the AV canal and the two ventricles over this same range (HH16–HH27), we saw that this same volume grew from 0.35 to 4.58 mm^3, which is similar in range to their data, although the absolute values likely reflect differences in measurement techniques. Stroke volume measurements used in the Hu and Clark study only assess the blood volume pumped through the chamber, not the entire cavity, and, therefore, will underestimate volume measurements. Hu and Clark also compared stroke volume with ventricular weight between HH16 and HH29 and found that both increase by approximately 10-fold over this period (Hu and Clark, 1989). Broekhuizen et al. also measured stroke volumes in developing chick ventricles between HH20 to HH35 and also found a 10-fold increase in volume during this time (0.14 to 1.28 mm^3; Broekhuizen et al., 1993). None of the aforementioned studies measured atrial, AV canal, or outflow tract volume. Taken together, our results show similar growth trends but differences in absolute magnitude. Because of the underestimating approximations that went into determining these reported volumes, we believe that the volumes presented in this study are more accurate.

It is unclear why chamber volumes in the heart during development are proportionally different from each other, but it may underlie differences in cardiac function over this period. The suction pump-like heart tube at HH12 loops between HH14 and HH18 and begins to accumulate secondary trabeculated myocardium between HH17 and HH20 (van den Hoff et al., 2001). Initially, the large majority of the early atrium is composed of that of the left with the right atrium emerging as a dextral expansion. This expansion is also concomitant with a dextral translation of the venous inflow. Previous research suggests that the AV canal is initially a large contributor to early cardiac volume, and similar to our quantitative measurements disappears as the valves form out of the primitive AV cushions (de la Cruz et al., 2001). It has been postulated that the slow conducting AV region loses mechanical stimulation with the development of the valves and, therefore, atrophies (Knaapen et al., 1995), but increased expansion and remodeling of the atria and ventricles is also a possible explanation (Oosthoek et al., 1998). Embryonic heart function is not identical to that of the adult, and, therefore, requires new experiments to understand these differences.

Micro-CT was also able to profile the 3D development of the atrioventricular valves and showed clearly the progression of the AV cushions into thin fibrous valves and interventricular septum. We show that the majority of the AV cushion mass contributes to the formation of the septal leaflet of the left AV, while the most dextral portion is absorbed into the developing muscular septum. The development of the mural leaflet appears to be formed in part by the development of AV myocardial fenestrations at HH27, which delaminate this cushion from the ventricular wall. The right AV valve in the chick becomes a muscular flap extending from the dextral myocardial wall, which was reflected in Micro-CT images. We also quantified the developing of ventricular trabeculation, and showed that the right ventricle becomes coarsely trabeculated in comparison to the left ventricle, which is in agreement with previous studies on developing myocardial architecture. The outflow tracts were also perfused in this study with good recreation of primitive cushions, but outflow valves were more difficult to completely perfuse because the pumping action of the beating hearts required to maintain physiological heart volumes cause this region to be regularly cleared of contrast polymer, especially at the small tortuous region of the distal outflow cushions. Perfusion of this region can be accomplished after perfusion of the heart chambers by injecting through the pulmonary artery and aorta, but it is important to attempt this before the polymer solidifies, otherwise localized regions of nonphysiological dilation will develop.

In summary, Micro-computed tomography can be used to image developing cardiovascular lumens and quantify 3D volumetric and morphologic parameters faster and less expensively than other techniques. Because the imaging process is nondestructive, samples are available for further analysis of gene and pro-

tein expression. The creation of more advanced contrast agents may permit the ability to gate and measure changing volumes over time, only increasing the utility of this technique.

EXPERIMENTAL PROCEDURES

Embryo Perfusion

Two-day incubated chick embryos were cracked into hexagonal weigh boats and placed inside 150-mm culture dishes with 50 ml of Earle's Balanced Salt Solution (EBSS). When placed into a 37°C incubator (no CO_2), this system enabled embryos to be cultured ex ovo for up to 8 additional days (HH36). Borosilicate glass capillary tubes (Sutter Instrument Co., OD 1.0 mm, ID 0.75 mm) were pulled into microneedles with inner diameters ranging from 20 to 80 μm, and then beveled to approximately 45 degrees using a microforge. Microneedles were then attached to small diameter silastic tubing (VWR, #63010-007) connected to a 5-ml syringe by means of a 20.5-gauge needle (Becton Dickinson). At specific stages of incubation between HH15 and HH36 (HH15,16,17,19,23,25,27,30,36), embryos and vitelline vasculature were removed from the egg yolk by severing the most distal portion of vessels with microscissors, and scooping the embryo out with a flat spoon. The embryo was then quickly placed in a culture dish with a small amount of EBSS to keep the embryo from drying out (but not enough to float). Embryos were then perfused with a polymerizing CT dense contrast agent at a ratio of 80: 15:5 diluent:agent:catalyst (Mirofil, Flow-Tech, Inc.). Perfusion was accomplished by positioning the syringe with a laboratory clamp/stand to create a gravity-driven pressure gradient. Depending on the stage of the embryo perfused, the height was adjusted between 5 cm (HH15) to 35 cm (HH36) in an approximately linear manner. The diameter of microneedle also increased with stage perfused (20 μm for HH15 to 80 μm for HH36) to maintain the flow rate of the perfusate and limit premature polymerization. Microneedle injection locations were to specific regions depending on stage of development. Tubular hearts (pre-HH26 hearts) were perfused through the vitelline vasculature, whereas later stage hearts were perfused directly through the ventricular walls. Beating heart embryos were perfused so that myocardial contraction allowed the clearance of excess polymer into the outflow tract and systemic vasculature. Perfusion reached completion in approximately 10 min, after which the needle was removed. The above ratio of contrast components resulted in polymerization into a cast approximately 10 min after perfusion, after which the embryos were fixed in 4% paraformaldehyde for 48 hr and then placed in phosphate buffered saline (PBS).

Micro-CT Scanning

The embryonic thoraxes with undisturbed hearts were placed into smaller cassettes to minimize total scan volume and filled with PBS. Embryonic hearts were imaged by using a VivaCT Micro-computed tomography scanner (Scanco Medical, Bassersdorf, Switzerland) at 10.5 μm resolution. The scan head revolves 360 degrees around the subject, imaging at discrete intervals to create a series of slices based on the CT dense polymer. The resulting set of images comprised the luminal space inside the heart at the different stages. Slices containing portions of the different chambers of the heart were traced manually by identifying a contour inclusive of that portion of the CT dense region contained within that chamber. The Scanco reconstruction software then assembles the outlined regions to render 3D volumes. Hearts before HH19 contained a single atrium and ventricle, but also an hourglass-shaped AV canal region between them. The outflow tract at these early stages was identified as beginning at the distal end of the single ventricle, and continuing until the arch artery branching. Later stage hearts contained both atria and ventricles, which were separated from each other by tracing along the budding interatrial and interventricular septa. The hearts were distinctively four chambered by HH30 (two atria and ventricles separated by AV valves), at which stage the outflow tract (volume between ventricles and outflow cushions) was almost nonexistent. This process was repeated for each segment/chamber of the heart with at least three hearts per developmental stage.

Computational Analyses

Volumetric and morphometric analyses were performed using direct distance transformation algorithms described previously for trabecular bone (Hildebrand and Ruegsegger, 1997; Hildebrand et al., 1999). Total lumen volume for each segment/chamber was calculated by tabulating the CT dense area of the traced region in each slice and then multiplying it by the thickness (10.5 μm). Trabeculation was quantified using well-established parameters used in trabeculated bone analyses. Trabecular number (TbN), thickness (TbTh), and spacing (TbSp) were determined by the Scanco software from the generated 3D directly. Trabecular number in the case of cardiac development refers to the density of identifiable trabeculae in a ventricular wall. Trabecular thickness refers to the diameter of a particular trabeculum, in this case a pit in the ventricular wall. Trabecular spacing denotes the average distance between trabecular pits. The computational algorithm works by generating point spheres within the selected volume (ventricle) that expand, intersecting trabeculae at defined radii to generated the aforementioned parameters. This process is routinely performed at 5- to 10-μm voxel size, which is appropriate for these studies. It is important to note that these parameters were determined from the chamber volume, not the tissue volume, so the interpretation of these parameters should be inverted to coincide with aspects of the tissue. These parameters were computed for each ventricle between stages 23 and 36. As before, at least three ventricles per developmental stage were analyzed.

Comparison with SEM and Serial Section Reconstruction

Additional hearts of identical stages were processed and analyzed using SEM (Sedmera et al., 1997, 1998) and serial section reconstruction. Serial section reconstruction was performed on HH17, HH24, and HH30 staged

hearts using frontal plane sections at 50-μm intervals. Digital images were taken of each section and calibrated with a scale of known length. Approximately 15–25 sections per heart were imaged. The images were then imported to AMIRA, and each image was rotated and/or translated in registration. Similar to the Micro-CT processing, the luminal space was identified on each section by manual trace. The AMIRA software then generated the luminal heart volume using a cubic splice interpolation between each section. These volumes were then compared with the Micro-CT–generated volumes and the SEM images for morphological accuracy.

ACKNOWLEDGMENTS

The authors thank Angela Lin for her technical assistance in Micro-CT scanning and processing. We also thank Tomas Pexieder in generating the HH17 SEM image. J.T.B. was funded by a NIH research training grant in pediatric cardiology, and R.R.M. was funded by NIH grants.

REFERENCES

Broekhuizen ML, Mast F, Struijk PC, van der Bie W, Mulder PG, Gittenberger-de Groot AC, Wladimiroff JW. 1993. Hemodynamic parameters of stage 20 to stage 35 chick embryo. Pediatr Res 34:44–46.

Chappard C, Peyrin F, Bonnassie A, Lemineur G, Brunet-Imbault B, Lespessailles E, Benhamou CL. 2006. Subchondral bone micro-architectural alterations in osteoarthritis: a synchrotron micro-computed tomography study. Osteoarthritis Cartilage 14:215–223.

Collins-Nakai R, McLaughlin P. 2002. How congenital heart disease originates in fetal life. Cardiol Clin 20:367–383, v–vi.

de la Cruz MV, Markwald RR, Krug EL, Rumenoff L, Sanchez Gomez C, Sadowinski S, Galicia TD, Gomez F, Salazar Garcia M, Villavicencio Guzman L, Reyes Angeles L, Moreno-Rodriguez RA. 2001. Living morphogenesis of the ventricles and congenital pathology of their component parts. Cardiol Young 11:588–600.

Duvall CL, Robert Taylor W, Weiss D, Guldberg RE. 2004. Quantitative microcomputed tomography analysis of collateral vessel development after ischemic injury. Am J Physiol Heart Circ Physiol 287:H302–H310.

Fong KW, Toi A, Salem S, Hornberger LK, Chitayat D, Keating SJ, McAuliffe F, Johnson JA. 2004. Detection of fetal structural abnormalities with US during early pregnancy. Radiographics 24:157–174.

Forouhar AS, Liebling M, Hickerson A, Nasiraei-Moghaddam A, Tsai HJ, Hove JR, Fraser SE, Dickinson ME, Gharib M. 2006. The embryonic vertebrate heart tube is a dynamic suction pump. Science 312:751–753.

Gittenberger-de Groot AC, Bartelings MM, Deruiter MC, Poelmann RE. 2005. Basics of cardiac development for the understanding of congenital heart malformations. Pediatr Res 57:169–176.

Gossl M, Zamir M, Ritman EL. 2004. Vasa vasorum growth in the coronary arteries of newborn pigs. Anat Embryol (Berl) 208: 351–357.

Groenendijk BC, Hierck BP, Vrolijk J, Baiker M, Pourquie MJ, Gittenberger-de Groot AC, Poelmann RE. 2005. Changes in shear stress-related gene expression after experimentally altered venous return in the chicken embryo. Circ Res 96: 1291–1298.

Guldberg RE, Ballock RT, Boyan BD, Duvall CL, Lin AS, Nagaraja S, Oest M, Phillips J, Porter BD, Robertson G, Taylor WR. 2003. Analyzing bone, blood vessels, and biomaterials with microcomputed tomography. IEEE Eng Med Biol Mag 22:77–83.

Guldberg RE, Lin AS, Coleman R, Robertson G, Duvall C. 2004. Microcomputed tomography imaging of skeletal development and growth. Birth Defects Res C Embryo Today 72:250–259.

Hildebrand T, Ruegsegger P. 1997. Quantification of bone microarchitecture with the structure model index. Comput Methods Biomed Engin 1:15–23.

Hildebrand T, Laib A, Muller R, Degueker J, Ruegsegger P. 1999. Direct three-dimensional morphometric analysis of human cancellus bone: microstructural data from spine, femur, iliac crest, and calcaneus. J Bone Miner Res 14:1167–1174.

Hu N, Clark EB. 1989. Hemodynamics of the stage 12 to stage 29 chick embryo. Circ Res 65:1665–1670.

Hu N, Connuck DM, Keller BB, Clark EB. 1991. Diastolic filling characteristics in the stage 12 to 27 chick embryo ventricle. Pediatr Res 29(Pt 1):334–337.

Jenkins M, Rothenberg F, Roy D, Nikolski V, Hu Z, Watanabe M, Wilson D, Efimov T, Rollins A. 2006. 4D embryonic cardiography using gated optical coherence tomography. Optics Express 14:736–748.

Keller BB, MacLennan MJ, Tinney JP, Yoshigi M. 1996. In vivo assessment of embryonic cardiovascular dimensions and function in day-10.5 to -14.5 mouse embryos. Circ Res 79:247–255.

Knaapen MW, Vrolijk BC, Wenink AC. 1995. Growth of the myocardial volumes of the individual cardiac segments in the rat embryo. Anat Rec 243:93–100.

Liebling M, Forouhar AS, Gharib M, Fraser SE, Dickinson ME. 2005. Four-dimensional cardiac imaging in living embryos via postacquisition synchronization of nongated slice sequences. J Biomed Opt 10:054001.

Moorman AF, De Boer PA, Ruijter JM, Hagoort J, Franco D, Lamers WH. 2000. Radio-isotopic in situ hybridization on tissue sections. Practical aspects and quantification. Methods Mol Biol 137:97–115.

Oosthoek PW, Wenink AC, Vrolijk BC, Wisse LJ, DeRuiter MC, Poelmann RE, Gittenberger-de Groot AC. 1998. Development of the atrioventricular valve tension apparatus in the human heart. Anat Embryol (Berl) 198:317–329.

Schneider JE, Bamforth SD, Farthing CR, Clarke K, Neubauer S, Bhattacharya S. 2003. Rapid identification and 3D reconstruction of complex cardiac malformations in transgenic mouse embryos using fast gradient echo sequence magnetic resonance imaging. J Mol Cell Cardiol 35:217–222.

Sedmera D, Pexieder T, Hu N, Clark EB. 1997. Developmental changes in the myocardial architecture of the chick. Anat Rec 248:421–432.

Sedmera D, Pexieder T, Hu N, Clark EB. 1998. A quantitative study of the ventricular myoarchitecture in the stage 21–29 chick embryo following decreased loading. Eur J Morphol 36:105–119.

Sedmera D, Reckova M, Bigelow MR, Dealmeida A, Stanley CP, Mikawa T, Gourdie RG, Thompson RP. 2004. Developmental transitions in electrical activation patterns in chick embryonic heart. Anat Rec A Discov Mol Cell Evol Biol 280:1001–1009.

Smith BR. 2001. Magnetic resonance microscopy in cardiac development. Microsc Res Tech 52:323–330.

Soufan AT, van den Hoff MJ, Ruijter JM, de Boer PA, Hagoort J, Webb S, Anderson RH, Moorman AF. 2004. Reconstruction of the patterns of gene expression in the developing mouse heart reveals an architectural arrangement that facilitates the understanding of atrial malformations and arrhythmias. Circ Res 95: 1207–1215.

van den Hoff MJ, Kruithof BP, Moorman AF, Markwald RR, Wessels A. 2001. Formation of myocardium after the initial development of the linear heart tube. Dev Biol 240:61–76.

Weninger WJ, Mohun T. 2002. Phenotyping transgenic embryos: a rapid 3-D screening method based on episcopic fluorescence image capturing. Nat Genet 30:59–65.

Wenink AC. 1992. Quantitative morphology of the embryonic heart: an approach to development of the atrioventricular valves. Anat Rec 234:129–135.

Zimmer EZ, Chao CR, Santos R. 1994. Amniotic sac, fetal heart area, fetal curvature, and other morphometrics using first trimester vaginal ultrasonography and color Doppler imaging. J Ultrasound Med 13:685–690.